Sixteenth International Conference on
Geometry, Integrability and Quantization
June 6–11, 2014, Varna, Bulgaria
Ivaïlo M. Mladenov, Andrei Ludu
and Akira Yoshioka, Editors
Avangard Prima, Sofia 2015, pp 282–300
doi: 10.7546/giq-16-2015-282-300

Geometry, Integrability and Quantization

GEOMETRIC MODELS FOR SECONDARY STRUCTURES IN PROTEINS

MAGDALENA TODA and BHAGYA ATHUKORALLAGE

Department of Mathematics and Statistics, Texas Tech University
79409 Lubbock, Texas USA

Abstract. This research is motivated by a study of special types of surfaces of revolution, using methods from differential geometry, elasticity theory and variational calculus. In particular, we present an elastic membrane model for the beta barrels in protein biology, via a certain *Generalized Willmore type* energy functional. We study the corresponding Euler–Lagrange equation, as well as a specific boundary value problem whose solutions are *Generalized Willmore surfaces of revolution*. We study the corresponding solutions both theoretically and numerically.

MSC: 53A05, 53A10, 74B20
Keywords: Helfrich energy, elastic membrane, surfaces of revolution

CONTENTS

1. The Generalized Willmore Energy, Elastic Surface Membranes and Applications to Biology 283
   1.1. Beta Barrels are Rotationally Symmetric Surfaces, But What is the True Shape of Beta Barrels? 283
   1.2. The Wilmore Bending Energy versus the Helfrich Energy 284
   1.3. What is the Equivalent of the Helfrich Energy for Rotationally Symmetric Beta Barrels? 286
2. The Generalized Willmore Equation 288
   2.1. The Generalized Willmore Equation for a Rotational Surface of Revolution of Profile $u(x)$ 292
   2.2. Numerical Results and Discussion 293
References 299

1. The Generalized Willmore Energy, Elastic Surface Membranes and Applications to Biology

This paper is based on a previous work [10] published by the present authors. We provided a model for the energy of secondary structures in proteins, which is a Willmore-type energy that is similar to the Helfrich energy from the model of lipid bilayers. We proposed a new model for beta barrels, as solutions of what we call the *Generalized Willmore Equation* (GWE). We thereby rejected older models of beta barrels (like a best-fit by one-sheeted hyperboloids, or twisted hyperboloids) and we accepted, as a particular and singular case, the catenoidal (minimal) model for beta barrels. We provided theoretical and experimental arguments in favor of new models for beta barrels, based on the Willmore-Helfrich type energy.

1.1. Beta Barrels are Rotationally Symmetric Surfaces, But What is the True Shape of Beta Barrels?

In biochemistry, biophysics and mathematical biology, secondary structures represent the main types of three-dimensional geometric shapes of local segments of biopolymers (e.g., proteins and nucleic acids (DNA/RNA). On a finer level - the atomic positions in three-dimensional space are said to form the tertiary structure. The secondary structure can be formally defined by the hydrogen bonds of the biopolymer, as observed in an atomic-resolution structure. In proteins, the secondary structure is defined by the patterns of hydrogen bonds between backbone amino and carboxyl groups. In nucleic acids, the secondary structure is defined by the hydrogen bonding between the nitrogenous bases. The most common secondary structures are the alpha helices. The second most-common are the beta sheets and beta barrels. A beta barrel is a collection of beta-sheets that twist and coil in a shape that can be described as a smooth surface of revolution which resembles a barrel. In this structure, the first strand is hydrogen bonded to the last. Beta-strands in beta-barrels are typically arranged in an antiparallel fashion. Barrel structures are commonly found in proteins that span cell membranes and in proteins that bind hydrophobic ligands in the barrel center.

Several models were proposed for beta sheets and beta barrels. Among them, we recall, in this chronological order: the twisted one-sheeted hyperboloid (see [7], 1984), followed by the usual one-sheeted hyperboloid (see [6], 1988), and much later, the catenoid as a best-fit (see [5], 2006). Over time, all the above-mentioned surfaces have been tried as "best models" for beta barrels. We became aware of the fact that none of these models is satisfactory, for various reasons: for a large diversity of aminoacids, the mean curvature was experimentally measured and it turned out to be close to a specific constant, which is small in absolute value, but not negligible (in particular, far enough from zero). For example, for the following

Table 1. Mean curvature values of beta barrels for several types of proteins (from [4]).

Protein	Average of mean curvature	Standard deviation of mean curvature
Triose phosphate isomerase	0.040	0.021
Taka-amylase	0.035	0.007
Glycolate-oxidase	0.035	0.007
Trimethanolamine dehydrogenase	0.037	0.013
Cytochrome b2	0.033	0.005
Aldolase	0.035	0.112

enzymes: glycolate-oxidase, taka-amylase, and aldolase, the mean curvature H, measured experimentally for beta-sheets, is approximately $H = 0.039$ (for each of them). Therefore, we have rejected the historical models one-by-one, and we tried to find answers among constant mean curvature (CMC) surfaces, and further, among Willmore surfaces. In [4], the authors presented the mean curvature values for different types of proteins, and are depicted in Table 1.

1.2. The Wilmore Bending Energy versus the Helfrich Energy

Classical differential geometry extensively studied minimal surfaces, which represent critical points of the Dirichlet energy. Soon after the minimal surface theory came into place, physicists and mathematicians devoted many studies to constant mean curvature surfaces, which realize a minimization of the surface area, with certain volume constraints. These studies did not answer all the questions regarding bending energy.

At the beginning of the 19th century, both Poisson and Sophie Germain proposed a model based on an energy of type

$$F = 2k_c \int_M H^2 \mathrm{d}S$$

for a solid elastic membrane of generic type, where H and $\mathrm{d}S$ represent respectively the mean curvature and the area element of the surface. The constant k_c is called bending modulus by some physicists and engineers. The generic Willmore energy, by definition, is given as

$$F = \int_M (H^2 - K)\mathrm{d}S.$$

Here K represents the Gaussian curvature. Note that the Poisson free energy and the Willmore energy are very closely related: for a closed surface M, the Gauss-Bonnet theorem states

$$\int_M K \mathrm{d}S = 2\pi\chi(M)$$

where $\chi(M)$ represents the Euler characteristic of the surface, that is a topological invariant. Further, the Willmore flow was introduced, as the flow corresponding to the Willmore energy (an L^2-gradient flow). Cell membranes tend to position themselves as to minimize the Helfrich energy (an extension of the classical Willmore energy). Actually, cell membranes are not at all a singular case: all the biological elastic membranes follow the rules of Willmore-type energy minimization, with or without additional constraints. Therefore, we can affirm that there exist many Willmore-type energies, leading us to the concept of generalized Willmore energy.

In 1973, Helfrich [3] proposed a model for the lipid bilayers based on a Willmore-like energy which represented a revolution in the study of cell membranes. Namely, he deduced the expression for the elastic energy of curvature per unit area of the membrane, as

$$g_c = (k/2)(2H - \mathbb{h})^2 + \bar{k}K$$

where $\mathbb{h}$ is the so called spontaneous curvature of the membrane surface.

The total bending energy of the membrane is given by the integral

$$\int_M g_c \, \mathrm{d}S.$$

The spontaneous curvature $\mathbb{h}$ is due to the "spontaneous splay" of the liquid crystals.

The constant k is the bending rigidity and $\bar{k}$ is the elastic modulus of the Gauss curvature K, and it is called by many "the second bending rigidity". Both these constants depend on the elastic constants and the thickness of the elastic membrane. This integral is called the Helfrich free energy of lipid bilayers or lipid membranes. He gave a rigorous proof for these equations, in terms of differential geometry (two-dimensional differential geometric invariants).

Helfrich and collaborators proposed that the equilibrium shape of a vesicle or red blood cell membrane be given by the critical point (minimum) of the following functional

$$(k/2)\int (2H - \mathbb{h})^2 \mathrm{d}S + \Delta P \int \mathrm{d}V + \gamma \int \mathrm{d}S$$

where k is the bending rigidity of the vesicle membrane, $\mathrm{d}S$ is the surface area element and $\mathrm{d}V$ is the volume element. The value ΔP represents the pressure difference between the inside and outside of the cell membrane, respectively (osmotic pressure). The value γ represents the tensile stress acting on the surface as surface tension.

The variation of the free Helfrich energy is straightforward to compute, and gives the following equation (its formula and some numerical applications were communicated by Ou-Yang and Helfrich [8] in 1989)

$$k\nabla_g^2(2H) - 2\gamma H + k(2H + \mathbb{h})(2H^2 - \mathbb{h}H - 2K) + \Delta P = 0.$$

Here, the operator ∇_g^2 is the Laplace operator (which depends on the metric g adopted on the surface).

Note that this Laplace-type equation is not easy to integrate, due to its high order, but many numerical solutions have already been computed for different boundary value problems. Its simplest solutions are the sphere and the circular cylinder, which in particular are CMC. Helfrich and Deuling provided a classification of numerically computed shapes, found by minimizing Helfrich's energy functional. Along the solutions, we note two exact solutions of great importance: the Clifford torus and the circular biconcave discoid, explaining the existing shapes of the red blood cells and other cells.

It is important to remark that boundary value problems for this equation are tractable as they involve all of the above: normal curvature, geodesic curvature and geodesic torsion of the boundary curve, summing up to four different equations, called the shape equation and the boundary conditions of lipid bilayers.

1.3. What is the Equivalent of the Helfrich Energy for Rotationally Symmetric Beta Barrels?

For micromolecular *sheets* (secondary structures such as alpha, beta or alpha-beta sheets), we proposed (see [10]) a model similar to that proposed by Helfrich for the cell biology. In our model, the term ΔP disappears, and the constant $\mathbb{h}$ highly depends on the solvent that is used for the protein molecule. On the other hand, the backbone (consisting of molecular chains of atoms) imposes an additional "backbone strain tensor" which can be represented by a 2×2 diagonal matrix A. Hence, the strain tensor changes the Helfrich-type equation into an equation of the following type (which we will call Willmore-Helfrich (W-H) equation for secondary structures in proteins)

$$k\Delta_g(2H) - 2\lambda H + k(2H + \mathbb{h})(2H^2 - \mathbb{h}H - 2K) + l(a_{11}k_1 + a_{22}k_2) = 0. \quad (1)$$

Here, $\Delta_g = \nabla_g^2$ represents the Laplace-Beltrami operator with respect to the Riemannian metric g, and k_1 and k_2 represent the principal curvatures of the surface M in *isothermic coordinates*. The coefficients a_{11} and a_{22} are the main diagonal entries of the strain tensor matrix.

An *isothermic parameterization* is a local surface immersion that is *isothermal* (i.e., the induced Riemannian metric has the property $g_{11} = g_{22}$ and $g_{12} = 0$),

and at the same time, in curvature-lines (that is, the metric and second fundamental forms are both diagonal). The categories of surfaces which admit isothermic parameterizations include but are not limited to: all rotational surfaces and all constant mean curvature surfaces.

In this context, k and l represent bending rigidities, just as in the cell-membrane models, while λ represents the new notion of tensile stress.

Observe that our recently proposed model is very far from the one-sheeted hyperboloid and twisted hyperboloid models, and it is also a lot more general than the minimal, catenoidal model. We had accepted the experimentally-observed fact that barrels have rotational symmetry, and we kept the beta sheet model as a surface of revolution, just as in the previous theories.

So, what are the rotationally-symmetric beta barrels that satisfy our W-H equation for secondary structures in proteins?

We have studied some of the solutions, both analytically and numerically, and they include parts (patches) of catenoids and unduloids.

For some types beta barrels, the catenoidal model is a very good model for practical purposes. But for others, like the CFP model represented in Fig. 1, the Delaunay unduloids certainly present a more appropriate model. To us, this was naturally expected for a long time, especially since the mean curvature of beta-barrels is far enough from zero for the case of many of the enzymes that were studied (e.g., see our Table 1).

Clearly, catenoids represent the only minimal surfaces of revolution, and in particular, they are Willmore surfaces. However, the true shape of the beta barrels consists of generalized Willmore surfaces of revolution. The catenoid is just a particular solution among all these shapes. One of our open problems under current investigation is to provide the necessary and sufficient conditions for the boundary value problem corresponding to a generalized Willmore equation which produces a perfect catenoid, versus a catenoidal-like $H \neq 0$ generalized Willmore surface of revolution. We would also like to mention a few important studies of the Willmore energy and related energies, and their multiple applications to physics and biology, which belong to Mladenov and his collaborators. We are hereby mentioning only a few of the most recent related articles [9, 11, 12]. As a relevant real-world application of high relevance and actuality, observe the model of the beta barrel of green fluorescent protein in Fig. 1 and remark its unduloidal shape (Delaunay unduloid). Martin Chalfie, Osamu Shimomura and Roger Y. Tsien were awarded the 2008 Nobel Prize in Chemistry on 10 October 2008 for their discovery and development of the GFP.

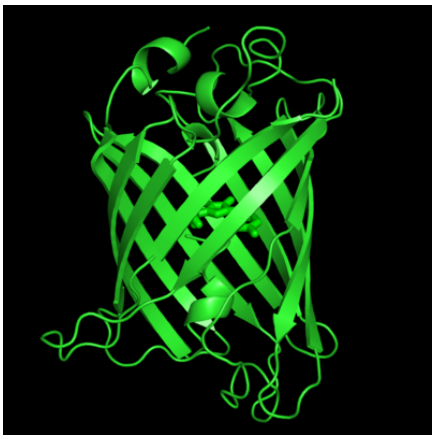

Figure 1. Beta Barrel of the GFP (*green fluorescent protein* isolated from jelly fish) by scientists Martin Chalfie, Osamu Shimomura and Roger Tsien - Nobel prize recipients (courtesy of the American Association of Clinical Chemistry).

2. The Generalized Willmore Equation

In this section, we introduce the notion of GWE, presented in our own acceptance and our own terminology. Actually, several recent papers use the term of Willmore-type energy to designate the Helfrich energy for lipid bilayers, and similar cases, in which bending rigidities are introduced as multiplicative constants of the mean curvature H and the Gaussian curvature K, while usually neglecting the superficial tension of the membranes. In our case, the generalized Willmore energy is a combination between the classical bending energy (Willmore energy) and the energy due to the superficial tension. The following is a proof of the GWE, in the spirit of the classical proof given by Willmore for the classical Willmore equation [13].

Theorem 1. *Assume M is a compact oriented surface, immersed in $\mathbb{R}^3$. Let E_w be the Generalized Willmore energy functional*

$$E_w = \int_M (kH^2 + \mu)\,\mathrm{d}S \tag{2}$$

where $k = 2k_c$ represents the double of the usual bending rigidity, while μ is the superficial tension coefficient. Then, the Euler-Lagrange equation of (2) *is*

$$\Delta H + 2(H^2 - K - \epsilon)H = 0. \tag{3}$$

In (3), $\epsilon = \frac{\mu}{k}$, and ΔH represents the Laplace-Beltrami operator (acting on H) corresponding to the naturally induced metric corresponding to the surface immersion map.

Proof: The following proof mimics that of Willmore's equation given in [13]. Let M has the parametrization $\mathbf{r}(u_1, u_2)$. Then, the unit outward normal $\mathbf{N}$ is

$$\mathbf{N} = \frac{\mathbf{r}_{u_1} \times \mathbf{r}_{u_2}}{|\mathbf{r}_{u_1} \times \mathbf{r}_{u_2}|} = \frac{\mathbf{r}_1 \times \mathbf{r}_2}{|\mathbf{r}_1 \times \mathbf{r}_2|}$$

where $\mathbf{r}_i = \frac{\partial \mathbf{r}}{\partial u_i}$ for $i = 1, 2$.

Let the components of the Riemannian metric be $g_{ij} = \langle \mathbf{r}_i, \mathbf{r}_j \rangle$. Thus the First Fundamental Form on M is

$$I = \sum_{i,j}^{2} g_{ij} \, \mathrm{d}u^i \mathrm{d}u^j$$

and the Second Fundamental Form on M is

$$II = -\langle \mathrm{d}\mathbf{N}, \mathrm{d}\mathbf{r} \rangle = \sum_{i,j}^{2} h_{ij} \, \mathrm{d}u^i \mathrm{d}u^j$$

where $h_{ij} = -\langle \mathbf{N}_i, \mathbf{r}_j \rangle = h_{ji}$ and $\mathbf{N}_i = \frac{\partial \mathbf{N}}{\partial u^i}$.
We denote the inverse of the matrix of (g_{ij}) by (g^{ij}). Then, the mean curvature vector $\mathbf{H}$ is given by

$$\mathbf{H} = \Big(\frac{1}{2} \sum_{i,j}^{2} g^{ij} h_{ij} \Big) \mathbf{N}.$$

Further, the surface area element on M is

$$\mathrm{d}S = \sqrt{\det(g_{ij})} \, \mathrm{d}u^1 \wedge \mathrm{d}u^2.$$

Recall that the equations of Gauss are

$$\mathbf{r}_{ij} = \sum \Gamma_{ij}^{k} \mathbf{r}_k + h_{ij} \mathbf{N}. \tag{4}$$

In (4), $\mathbf{r}_{ij} = \frac{\partial^2 \mathbf{r}}{\partial u^i \partial u^j}$ and Γ_{ij}^{k} are the classical Christoffel symbols.
The Weingarten equations are

$$\mathbf{N}_i = -\sum h_i^j \mathbf{r}_j$$

where $h_i^j = g^{jk} h_{ki}$.
Let us consider a normal variation of the immersion given by

$$\bar{\mathbf{r}}(u^1, u^2, t) = \mathbf{r}(u^1, u^2) + t\phi(u^1, u^2)\mathbf{N}$$

where ϕ is a smooth real-valued function, and $t \in \big(-\frac{1}{2}, \frac{1}{2}\big)$. We denote by δ the operator $\frac{\partial}{\partial t}\big|_{t=0}$.

We introduce the following terminology: we say that M is a generalized Willmore surface if it satisfies the equation

$$\delta \int (kH^2 + \mu)\, \mathrm{d}S = 0. \tag{5}$$

The normal variation can be written as

$$\delta\bar{\mathbf{r}} = \phi\mathbf{N}, \qquad \delta\mathbf{r}_i = \phi_i\mathbf{N} + \phi\mathbf{N}_i.$$

Further

$$\begin{aligned}\bar{g}_{ij} &= \langle \mathbf{r}_i + t\phi_i\mathbf{N} + t\phi\mathbf{N}_i, \mathbf{r}_j + t\phi_j\mathbf{N} + t\phi\mathbf{N}_j\rangle \\ &= g_{ij} + t\phi\langle \mathbf{r}_i, \mathbf{N}_j\rangle + t^2\phi_i\phi_j + t\phi\langle \mathbf{N}_i, \mathbf{r}_j\rangle + t^2\langle \mathbf{N}_i, \mathbf{N}_j\rangle\end{aligned}$$

that yields the relation

$$\delta g_{ij} = -\phi \sum g_{ik}h^k_j - \phi g_{jk}h^k_i = -2\phi h_{ij}.$$

Hence

$$\delta g^{ij} = 2\phi g^{jk}h^i_k.$$

Let the area element be $W = \sqrt{\det(g_{ij})}$. Then

$$2W\frac{\partial W}{\partial t} = \sum \frac{\partial g_{ij}}{\partial t}W^2 g^{ij}.$$

Hence

$$\delta W = \sum \frac{1}{2}\delta g_{ij} W g^{ij} = \sum \frac{1}{2}(-2\phi W h_{ij}g^{ij}) = -2\phi HW.$$

Next, we compute $\delta\mathbf{N}$. Since, $\langle \mathbf{N}, \mathbf{r}_i\rangle = 0$, we have

$$\langle \delta\mathbf{N}, \mathbf{r}_i\rangle + \langle \mathbf{N}, \delta\mathbf{r}_i\rangle = 0.$$

Moreover

$$\langle \delta\mathbf{N}, \mathbf{r}_i\rangle = -\langle \mathbf{N}, \phi_i\mathbf{N} + \phi\mathbf{N}_i\rangle = -\phi_i.$$

Since $\langle \mathbf{N}, \mathbf{N}\rangle = 1$, we have that $\langle \delta\mathbf{N}, \mathbf{N}\rangle = 0$. We write $\delta\mathbf{N} = \sum b^j\mathbf{r}_j$. Then,

$$b^i = -g^{ij}\phi_j$$

and hence,

$$\delta\mathbf{N} = -g^{ij}\phi_j\mathbf{r}_i.$$

From the Gauss equation, we have

$$\langle \delta\mathbf{N}, \mathbf{r}_{ij}\rangle = -\langle g^{pq}\phi_q\mathbf{r}_p, \Gamma^k_{ij}\mathbf{r}_k\rangle = -\phi_k\Gamma^k_{ij}.$$

We now wish to obtain the formula

$$\langle \mathbf{N}, \delta\mathbf{r}_{ij}\rangle = \phi_{ij} - \phi h^k_i h_{jk}.$$

Observe that

$$\begin{aligned}\bar{\mathbf{x}} &= \mathbf{x} + t\phi\mathbf{N}, \qquad \bar{\mathbf{x}}_i = \mathbf{x}_i + t(\phi\mathbf{N}_i + \phi_i\mathbf{N})\\ \bar{\mathbf{x}}_{ij} &= \mathbf{x}_{ij} + t(\phi_{ij}\mathbf{N} + \phi_i\mathbf{N}_j + \phi_j\mathbf{N}_i + \phi\mathbf{N}_{ij}).\end{aligned}$$

Hence

$$\delta\mathbf{r}_{ij} = \phi_{ij}\mathbf{N} + \phi_i\mathbf{N}_j + \phi_j\mathbf{N}_i + \phi\mathbf{N}_{ij}$$

which gives

$$\begin{aligned}\langle\mathbf{N}, \delta\mathbf{r}_{ij}\rangle &= \phi_{ij} + \phi\langle\mathbf{N}, \mathbf{N}_{ij}\rangle = \phi_{ij} - \phi\langle\mathbf{N}_i, \mathbf{N}_j\rangle\\ &= \phi_{ij} - \phi\langle h_i^p\mathbf{r}_p, h_j^q\mathbf{r}_q\rangle = \phi_{ij} - \phi h_{ik}h_j^k c\end{aligned}$$

as required. We recall that $\langle\mathbf{N}, \mathbf{r}_{ij}\rangle = h_{ij}$. Hence

$$\begin{aligned}\delta h_{ij} &= \langle\delta\mathbf{N}, \mathbf{r}_{ij}\rangle + \langle\mathbf{N}, \delta\mathbf{r}_{ij}\rangle = -\phi_k\Gamma_{ij}^k + \phi_{ij} - \phi h_i^k h_{jk}\\ &= \nabla_i\nabla_j\phi - \phi h_i^k h_{jk}.\end{aligned}$$

Now, at last, apply δ to our integral. We have

$$\begin{aligned}\delta H &= \delta\Big(\frac{1}{2}g^{ij}h_{ij}\Big) = \frac{1}{2}\left(\delta g^{ij}\right)h_{ij} + \frac{1}{2}g^{ij}\left(\delta h_{ij}\right)\\ &= \frac{1}{2}2\phi g^{jk}h_k^i h_{ij} + \frac{1}{2}g^{ij}\left(\nabla_i\nabla_j\phi - \phi h_i^k h_{kj}\right)\\ &= \frac{1}{2}\left(\Delta\phi + \phi h_k^i h_i^k\right).\end{aligned}$$

The matrix (h_k^i) has as eigenvalues the principal curvatures κ_1 and κ_2.
Hence

$$h_k^i h_i^k = \operatorname{trace}(h^2) = \kappa_1^2 + \kappa_2^2 = 4H^2 - 2K.$$

Therefore, we get

$$2\delta H = \Delta\phi + \phi(4H^2 - 2K).$$

Let us now consider the following first variation

$$\delta\int(kH^2 + \mu)\,\mathrm{d}S = \int(2kH\delta H)\,\mathrm{d}S + \int(kH^2 + \mu)\delta(\mathrm{d}S).$$

We further need to take into consideration the formula

$$\delta W = -2\phi HW$$

in which we replace W by $\mathrm{d}S$. Replacing into the first variation on the integral above, we further obtain

$$\int(kH^2 + \mu)\,\delta(\mathrm{d}S) = \int(kH^2 + \mu)(-2\phi H)\,\mathrm{d}S.$$

Since M is a closed surface, it follows from the Green's theorem that

$$\int H\Delta\phi \,\mathrm{d}S = \int \phi\Delta H \,\mathrm{d}S.$$

Thus, we get

$$\delta \int (kH^2 + \mu)\,\mathrm{d}S = \int \phi\big(k\Delta H + kH(4H^2 - 2K) - 2H(kH^2 + \mu)\big)\,\mathrm{d}S.$$

This further gives the following Euler-Lagrange equation (after dividing by the factor k)

$$\Delta H + 2(H^2 - K - \epsilon)H = 0 \tag{6}$$

where $\epsilon = \frac{\mu}{k} = \frac{\mu}{2k_c}$ is a positive constant.

■

In a similar way, one can consider the case of a surface (membrane) with prescribed boundary, then consider the generalized Willmore type energy, and obtain the Euler-Lagrange equation together with the boundary conditions. We obtain that the condition $H = 0$ is the natural condition along the boundary

$$\begin{aligned} \Delta H + 2(H^2 - K)H - \frac{\mu}{k_c}H &= 0 \quad \text{on the surface} \\ H|_C &= 0 \quad \text{on } C \end{aligned} \tag{7}$$

which, as before, can be written as

$$\Delta H + 2(H^2 - K - \epsilon)H = 0$$

where $\epsilon = \frac{\mu}{2k_c}$ is a positive constant. As before H and K are the mean curvature and the Gauss curvature of the surface, respectively.

2.1. The Generalized Willmore Equation for a Rotational Surface of Revolution of Profile $u(x)$

Consider the GWE

$$\Delta H + 2(H^2 - k - \epsilon)H = 0 \tag{8}$$

for a surface of revolution that has the parametrization

$$\mathbf{r}(x, \varphi) = (x, u(x)\cos\varphi, u(x)\sin\varphi)$$

where $u(x)$ is the profile curve of the surface, and φ is the angle measured from the $xy-$plane in the counter clockwise direction. Then the corresponding Laplace-Beltrami operator is

$$\Delta H = \Delta_g H = \frac{1}{u\sqrt{1+u'^2}}\frac{\mathrm{d}}{\mathrm{d}x}\left(\frac{u}{\sqrt{1+u'^2}}\frac{\mathrm{d}H}{\mathrm{d}x}\right). \tag{9}$$

Moreover

$$H = \frac{-u''}{2(1+u'^2)^{3/2}} + \frac{1}{2u\sqrt{1+u'^2}} \tag{10}$$

and

$$K = \frac{-u''}{u(1+u'^2)^2}.$$

Hence, one may express K in terms of the functions H and u, in the following form

$$K = \frac{2}{u\sqrt{1+u'^2}}\left(H - \frac{1}{2u\sqrt{1+u'^2}}\right). \tag{11}$$

By using (9) and (11), we rewrite (8) to get

$$\frac{\mathrm{d}}{\mathrm{d}x}\left(\frac{u}{\sqrt{1+u'^2}}\frac{\mathrm{d}H}{\mathrm{d}x}\right) + 2H(H^2 - K - \epsilon)u\sqrt{1+u'^2} = 0$$

$$\frac{\mathrm{d}}{\mathrm{d}x}\left(\frac{u}{\sqrt{1+u'^2}}\frac{\mathrm{d}H}{\mathrm{d}x}\right) \tag{12}$$

$$+2Hu\sqrt{1+u'^2}\left(H^2 - \frac{2}{u\sqrt{1+u'^2}}\left(H - \frac{1}{2u\sqrt{1+u'^2}}\right) - \epsilon\right) = 0$$

and finally

$$\frac{\mathrm{d}}{\mathrm{d}x}\left(\frac{u}{\sqrt{1+u'^2}}\frac{\mathrm{d}H}{\mathrm{d}x}\right) + 2H\left((H^2-\epsilon)u\sqrt{1+u'^2} - 2H + \frac{1}{u\sqrt{1+u'^2}}\right) = 0.$$

Observe that (10) can be expressed in divergence form as

$$\frac{\mathrm{d}}{\mathrm{d}x}\left(\frac{-u'}{\sqrt{1+u'^2}}\right) = 2H - \frac{1}{u\sqrt{1+u'^2}}. \tag{13}$$

2.2. Numerical Results and Discussion

In order to obtain numerical solutions to GWE, we apply the commercial software COMSOL Multiphysics®. This is a finite element analysis, solver and simulation software (FEA Software package for various physics and engineering applications, especially coupled phenomena, or multiphysics). COMSOL Multiphysics also offers an extensive interface to MATLAB and its toolboxes for a large variety of programming, preprocessing and postprocessing possibilities.

There are physics-based modules with augment the core physics interfaces of COMSOL Multiphysics and provide additional interfaces for electrical, mechanical, fluid flow, and chemical applications. COMSOL Multiphysics represents a very powerful, and highly performant tool for PDEs like the boundary value problems associated to our GWE.

In order to use this tool, the GWE equation has to be put in divergence form, or as close as possible to divergence form. This is what we are performing in the following.

Recasting the equations (12) and (13), one can obtain

$$\frac{\mathrm{d}}{\mathrm{d}x}\left(\frac{-u}{\sqrt{1+u'^2}}\frac{\mathrm{d}H}{\mathrm{d}x}\right) - 2H\frac{1}{u\sqrt{1+u'^2}} = 2H\left((H^2-\epsilon)u\sqrt{1+u'^2} - 2H\right)$$
$$\frac{\mathrm{d}}{\mathrm{d}x}\left(\frac{-1}{\sqrt{1+u'^2}}\frac{\mathrm{d}u}{\mathrm{d}x}\right) = 2H - \frac{1}{u\sqrt{1+u'^2}}$$

which can be rewritten in the matrix form

$$\nabla\cdot\left(\begin{pmatrix}\frac{-u}{\sqrt{1+u'^2}} & 0\\ 0 & \frac{-1}{\sqrt{1+u'^2}}\end{pmatrix}\nabla\mathbf{u}\right) + \begin{pmatrix}\frac{-2}{u\sqrt{1+u'^2}} & 0\\ 0 & 0\end{pmatrix}\mathbf{u}$$
$$= \begin{pmatrix}2H\left((H^2-\epsilon)u\sqrt{1+u'^2} - 2H\right)\\ 2H - \frac{1}{u\sqrt{1+u'^2}}\end{pmatrix}.$$

Note that, $\mathbf{u} = \begin{pmatrix}H\\ u\end{pmatrix}$.

With our GWE rewritten in this divergence-type matrix form, we are now ready to use COMSOL Multiphysics as a solver.

By considering the interval $[-1,1]$, we numerically solve the system of equations (12) and (13) for the profile curve $u(x)$ with the following boundary conditions

$$u(\pm 1) = \alpha \qquad \text{and} \qquad H(\pm 1) = 0. \tag{14}$$

We refer to this boundary value problem as BGWE.

Considering fixed α and fixed ϵ values, profile curves are computed using COMSOL Multiphysics software and the corresponding profiles are shown in Figures 4, 5 and 6. Such a boundary value problem was considered for the classical Willmore surface of revolution by [1]. Remark that these boundary value conditions (of type Dirichlet and Navier, respectively) were proved to be the most natural conditions when it came to Willmore surfaces of revolution, by the authors of [1]. These authors studied some specific surfaces of revolution, using linearization around the Clifford torus. For the GWE, such a linearization procedure is not applicable in general. However, COMSOL Multiphysics is a general and powerful tool in solving any type of boundary value problem that is well-posed, for our GWE or equations of the same type (highly non-linear) - and not just for the rotationally invariant solutions of the classical Willmore equation.

While studying the Dirichlet-Navier boundary value problem for the classical Willmore equation (case $\epsilon = 0$), COMSOL provides the following one-parameter family of solutions (parameterized upon the value of the real parameter α, the "height" from the Dirichlet boundary condition).

When analyzing the graphs in Fig. 2, one can conclude that this value is close to 1.5 for the case when $\epsilon = 0$. After noting that the first minimal solution appears around the value $\alpha = 1.5$, we would like to establish for sure if such a threshold value exists, and if so, what its exact value would represent from a geometric and analytic viewpoint.

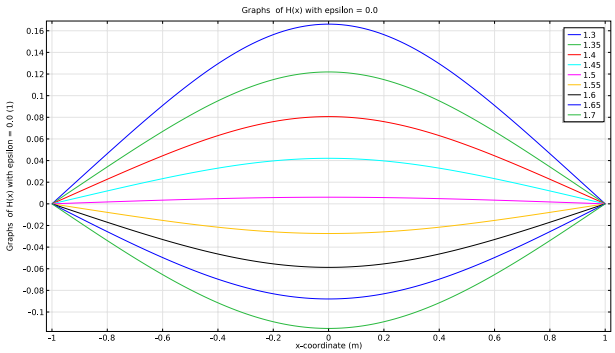

Figure 2. Solutions $H(x)$ to the BGWE for different α values of $\epsilon = 0$ (classical Willmore case).

We analytically searched for the smallest value of $\alpha = \alpha^*$ for which the generalized Willmore equation (GWE) admits a minimal solution (that is, with $H(x) = 0$ identically on the interval $[-1, 1]$).

Theorem 2. *Consider a Cartesian system of axes of coordinates x, y, z in $\mathbb{R}^3$ and the circles C_1, C_2 of the same radius α, centered at $(-1, 0, 0)$ and $(1, 0, 0)$, situated in planes orthogonal to the x-axis.*

Consider all regular surfaces of revolution of annular-type with boundary $C_1 \cup C_2$. Assume that among all these surfaces, there exists at least a surface M minimizing the generalized Willmore energy. This surface in assumed embedded in $\mathbb{R}^3$ and admitting the representation

$$M := \{(x, u(x)\cos\varphi, u(x)\sin\varphi)\ ;\ x \in [-1, 1],\ \varphi \in \mathbb{R}\}$$

with some function $u \in C^4([-1, 1], (0, \infty))$.

Then, the surface M is a solution of the following boundary value problem

$$\Delta H + 2H(H^2 - K - \epsilon) = 0 \quad \text{on } M \quad \text{where} \quad \epsilon = \frac{\mu}{k} \tag{15}$$

$$\partial M = C_1 \cup C_2, \quad H = 0 \quad \text{on} \quad \partial M,\ u(\pm 1) = \alpha. \tag{16}$$

Moreover: *there exists a positive value* α^* *(*$\alpha^* \approx 1.5089$*) that is independent from the value of* ϵ*, such that*

a) *If* $0 < \alpha < \alpha^*$*, then GWE admits NO minimal solution, that is, any solution satisfies:* $H = 0$ *on* ∂M *and* $H \neq 0$ *on* $M \setminus \partial M$.

b) *If* $\alpha = \alpha^*$*, then GWE admits exactly one minimal solution* (*a unique catenoid that exclusively depends on* α^*).

c) *If* $\alpha > \alpha^*$*, then GWE admits exactly two minimal solutions* (*two catenoids whose equations exclusively depend on* α).

Proof: The first part of the theorem directly follows from the proof of Theorem 1. The last part of the theorem, that is, the existence of α^*, follows by analyzing eventual minimal solutions. Containing: If a minimal solution to this problem exists, it will have to be a catenoid of the standard type: $y(t, x) = \frac{\cosh t}{t}$, where $t > 0$. Due to the endpoint values $x = \pm 1$, any such solution must verify the equation

$$\alpha = \frac{\cosh(t)}{t}. \tag{17}$$

We therefore study the intersections between the graphs of $f(t) = \cosh t$ and $g(t) = \alpha\, t$, for every fixed value of the real positive parameter α. Remark that $g(t) = \alpha\, t$ represents a pencil of lines, which contains a unique line that is tangent to $f(t)$ (for $\alpha = \alpha^* \approx 1.5089$) and for values $\alpha > \alpha^*$ each line in the pencils intersects $f(t)$ exactly twice.

Therefore, we conclude that we have the following three cases

i) If $0 < \alpha < \alpha^* = 1.5089$, the graphs $y(t) = \cosh t$ and $y(t) = \alpha\, t$, respectively have no intersections. Hence, there are no catenoidal solutions for GWE.

ii) If $\alpha = \alpha^* = 1.5089$, the graphs $y(t) = \cosh t$ and $y(t) = \alpha\, t$ exactly one intersection, at some value t_0. Therefore, GWE admits exactly one catenoid as solution.

iii) If $\alpha > \alpha^* = 1.5089$, the graphs $y(t) = \cosh t$ and $y(t) = \alpha\, t$ have exactly two intersections (at t_1 and t_2). Therefore, GWE admits two catenoidal solutions.

■

Further, we would like to analyze the α-family of solutions that corresponds to various fixed values of ϵ. We were able to construct corresponding families of solutions using COMSOL. It is very important to realize that, due to the nature of the numerical computations, only one minimal solution will appear in the numerically represented family of solutions (α-flow) (see $H = 0$ and its corresponding

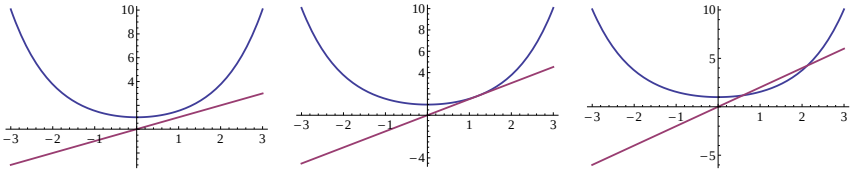

(a) No solutions: $\alpha < \alpha^*$ (b) Exactly one solution: $\alpha = \alpha^* \approx 1.5089$ (c) Two distinct solutions: $\alpha > \alpha^*$

Figure 3. Graphs of $f(t) = \cosh t$ (Blue) and $g(t) = \alpha\, t$ (Red) (in online version).

profile curve u). In the previous theorem, we just proved that at the threshold value ($\alpha = \alpha^*$) we always have a minimal solution, while for values larger than the threshold value $\alpha > \alpha^*$ we will always have two minimal solutions, corresponding to two different catenoidal profiles. Due to the nature of the numerical flow of solutions parameterized in time upon the parameter α, only a single catenoidal profile will be graphed in the flow of numerical solutions (see figures below for a better understanding on this issue). On the other hand, of course, each solution

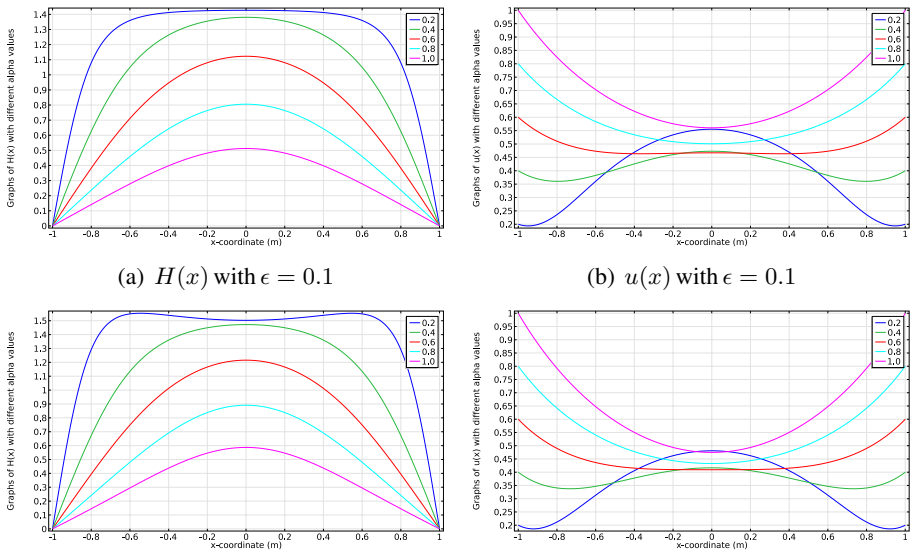

(a) $H(x)$ with $\epsilon = 0.1$ (b) $u(x)$ with $\epsilon = 0.1$

(c) $H(x)$ with $\epsilon = 0.5$ (d) $u(x)$ with $\epsilon = 0.5$

Figure 4. Solutions to *BGWE* as $H(x)$, and corresponding profile curves $u(x)$ for different α values and for fixed ϵ value.

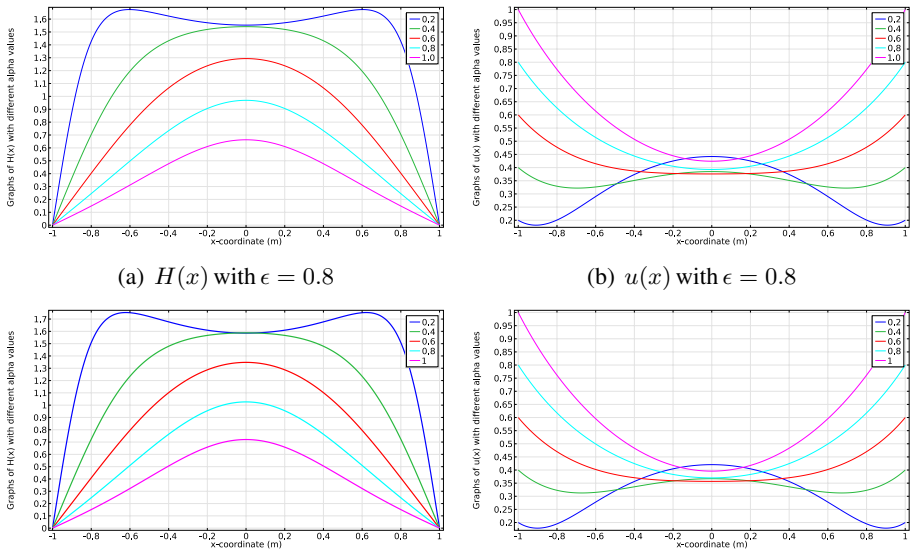

(a) $H(x)$ with $\epsilon = 0.8$ (b) $u(x)$ with $\epsilon = 0.8$

(c) $H(x)$ with $\epsilon = 1$ (d) $u(x)$ with $\epsilon = 1$

Figure 5. Solutions to *BGWE* as $H(x)$, and corresponding profile curves $u(x)$ for different α values and for fixed ϵ value.

to the BGWE (and in particular each catenoidal solution) can actually be represented in COMSOL, if we chose the unique value α appropriately, and deal with the solution branching (in order to graph all corresponding solutions u if that is the case).

Remark the shapes obtained for the profile $u(x)$ as solutions to BWGE in all the figures presented in this paper: they resemble either a catenary, or an undulary - thus generating catenoidal and unduloidal Generalized Willmore surfaces of revolution. Due to the physical nature of our Dirichlet-Navier boundary value problem for GWE, the nodoidal solutions are absent, but nodoidal solutions would certainly be present for other types of boundary value conditions of the GWE.

Following our analysis, for each and every value of α that is above α^*, there exist three distinct solutions, namely two catenoidal profiles and a non-minimal solution - which could be unstable (that is, not a local minimizer of the energy). Remark that catenoids represent global minimizers, as Deckelnick and coauthors [2] showed in a recent paper. For the classical Willmore case $\epsilon = 0$, authors proved that the non-minimal solution is contained between the two catenoids, and it is unstable. Our numerical analysis on the stability of the solutions to the GWE is in progress.

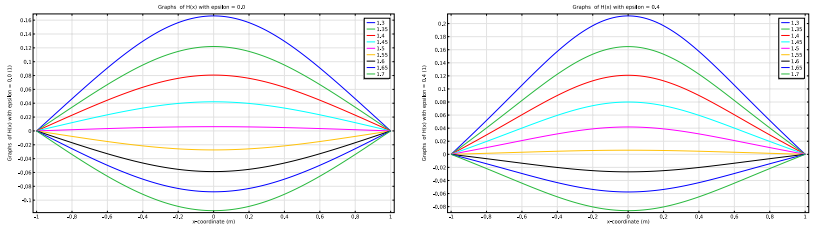

(a) $H(x)$ with $\epsilon = 0.0$ (b) $H(x)$ with $\epsilon = 0.4$

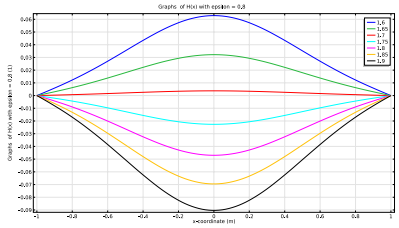

(c) $H(x)$ with $\epsilon = 0.8$

Figure 6. Mean curvature graphs with for $\epsilon = 0, 0.4, 0.8$.

References

[1] Dall'Acqua A., Deckelnick K. and Grunau H.-C., *Classical Solutions to the Dirichlet Problem for Willmore Surfaces of Revolution*, Adv. Calc. Var. **1** (2008) 379–397.

[2] Deckelnick K. and Grunau H.-C., *A Navier Boundary Value Problem for Willmore Surfaces of Revolution*, Analysis **29** (2009) 229–258.

[3] Helfrich W., *Elastic Properties of Lipid Bilayers*: *Theory and Possible Experiments*, Z. Naturforsch c **28** (1973) 693–703.

[4] Koh E. and Kim T., *Minimal Surface as a Model of $\beta-$Sheets*, Proteins: Structure, Function and Bioinformation, **61** (2005) 559–569.

[5] Koh E., Kim T. and Cho H.-S., *Mean Curvature as a Major Determinant of β-Sheet Propensity*, Bioinformatics **22** (2006) 297–302.

[6] Lasters I., Wodak S., Alard P. and Cutsem E., *Structural Principles of Parallel Beta-Barrels in Proteins*, Proc. Natl. Acad. Sci. **85** (1988) 3338–3342.

[7] Novotný J., Bruccoleri R. and Newell J., *Twisted Hyperboloid* (*Strophoid*) *as a Model of Beta-Barrels in Proteins*, J. Mol. Biol. **177** (1984) 567–573.

[8] Ou-Yang Z.-C. and Helfrich W., *Bending Energy of Vesicle Membranes*: *General Expressions for the First, Second and Third Variation of the Shape Energy and Applications to Spheres and Cylinders*, Phys. Rev. A **39** (1989) 5280-5288.

[9] Pulov V., Hadzhilazova M. and Mladenov I., *Symmetries and Some Special Solutions of the Helfrich Model*, In: Similarity and Symmetry Methods, J.-F. Ganghoffer and I. Mladenov (Eds), Springer, Berlin 2014, pp 353–364.

[10] Toda M. and Athukorallage B., *Geometry of Biological Membranes and Willmore Energy*, AIP Conf. Proc. **1558** (2013) 883–886.

[11] Vassilev V. and Mladenov I., *Geometric Symmetry Groups, Conservation Laws and Group-Invariant Solutions of the Willmore Equation*, Geometry, Integrability and Quantization **5** (2004) 246-265.

[12] Vassilev V., Djondjorov P. and Mladenov I., *Lie Group Analysis of the Willmore and Membrane Shape Equations*, In: Similarity and Symmetry Methods, J.-F. Ganghoffer and I. Mladenov (Eds), Springer, Berlin 2014, pp 365–376.

[13] Willmore T., *Riemannian Geometry*, Clarendon Press, Oxford 1996.